Angewandte Chemie
Eine Zeitschrift der Gesellschaft Deutscher Chemiker

Supporting Information

Fragment-Based Stabilizers of Protein–Protein Interactions through Imine-Based Tethering

Madita Wolter[+], Dario Valenti[+], Peter J. Cossar, Laura M. Levy, Stanimira Hristeva, Thorsten Genski, Torsten Hoffmann, Luc Brunsveld, Dimitrios Tzalis, and Christian Ottmann**

anie_202008585_sm_miscellaneous_information.pdf

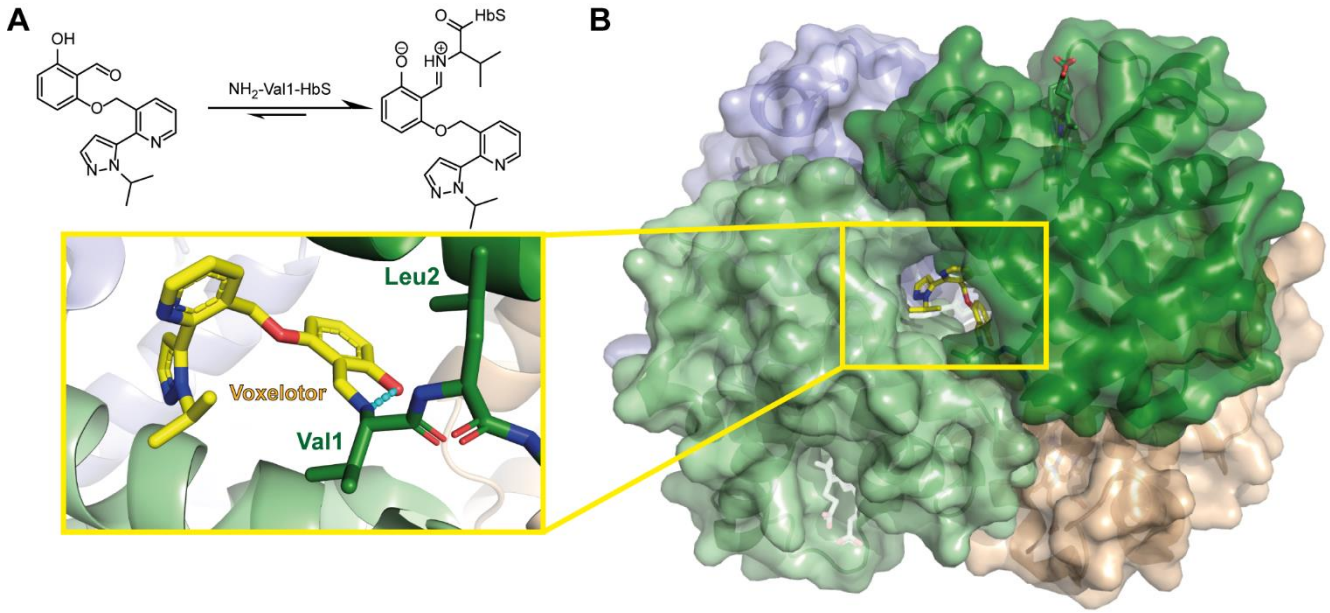

Figure S1: Example of a trapping moiety stabilizing an aldimine bond. (A) Voxelotor binds to the N-terminal amine of the hemoglobin mutant HbS via imine formation. The 2-hydroxy of the benzaldehyde ring stabilizes the imine bond by intramolecular salt bridge formation. **(B)** Crystal structure of Voxelotor (yellow sticks) binding to Val1 of HbS monomer (green sticks, overview shows three additional monomers shown as pale green, pale blue and beige surface)(PDB ID: 5E83). The intramolecular salt bridge is indicated with cyan dashes. A second Voxelotor binding to the pale green HbS monomer in the same interface pocket is hidden for clarity.

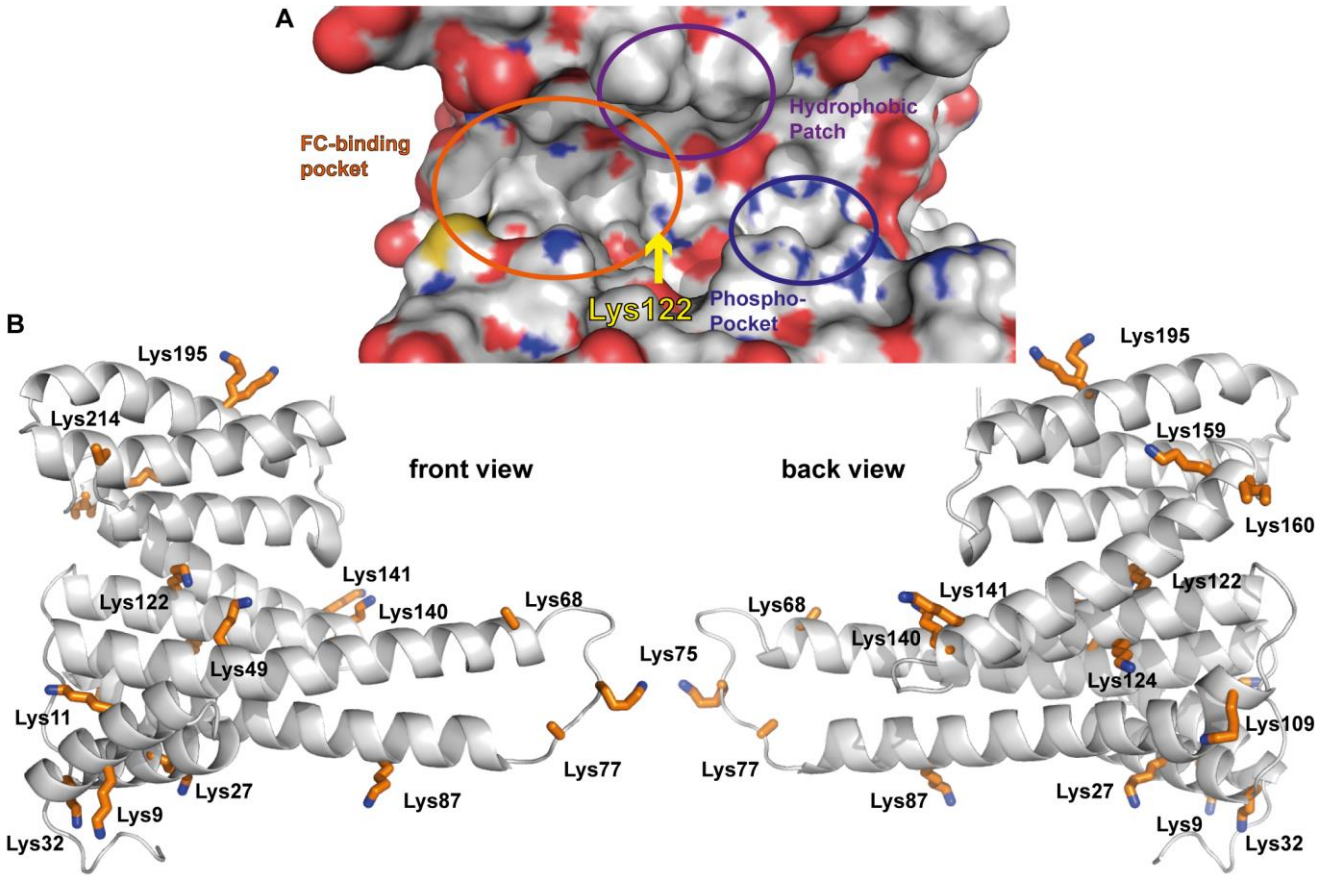

Figure S2: Analysis of 14-3-3 amino acid composition. (A) Binding groove of 14-3-3σ C Van-der-Waals surface of 14-3-3σ. Circles indicated the phospho-binding pocket of 14-3-3, a hydrophobic patch next to the phospho-binding site and the binding pocket of the fusicoccin class of natural compounds. (B) Orientation of the 18 lysine residues of 14-3-3σ.

Table S1: Analysis of pKa values of lysine residues based on the p65_45^{R}/14-3-3σΔC crystal structure.

	p65/14-3-3σΔC

#Fields: Residue N Chain	IpKa	pKa
LYS 9 A	10.4	10.2
LYS 11 A	10.4	11.3
LYS 27 A	10.4	11.2
LYS 32 A	10.4	10.6
LYS 49 A	10.4	10.6
LYS 68 A	10.4	11.2
LYS 75 A	10.4	10.5
LYS 77 A	10.4	10.2
LYS 87 A	10.4	10.3
LYS 109 A	10.4	10.5
LYS 122 A	**10.4**	**10**
LYS 124 A	10.4	10.4
LYS 140 A	10.4	10.5
LYS 141 A	10.4	11.2
LYS 159 A	**10.4**	**10**
LYS 160 A	10.4	11
LYS 195 A	10.4	10.8
LYS 214 A	10.4	10.7

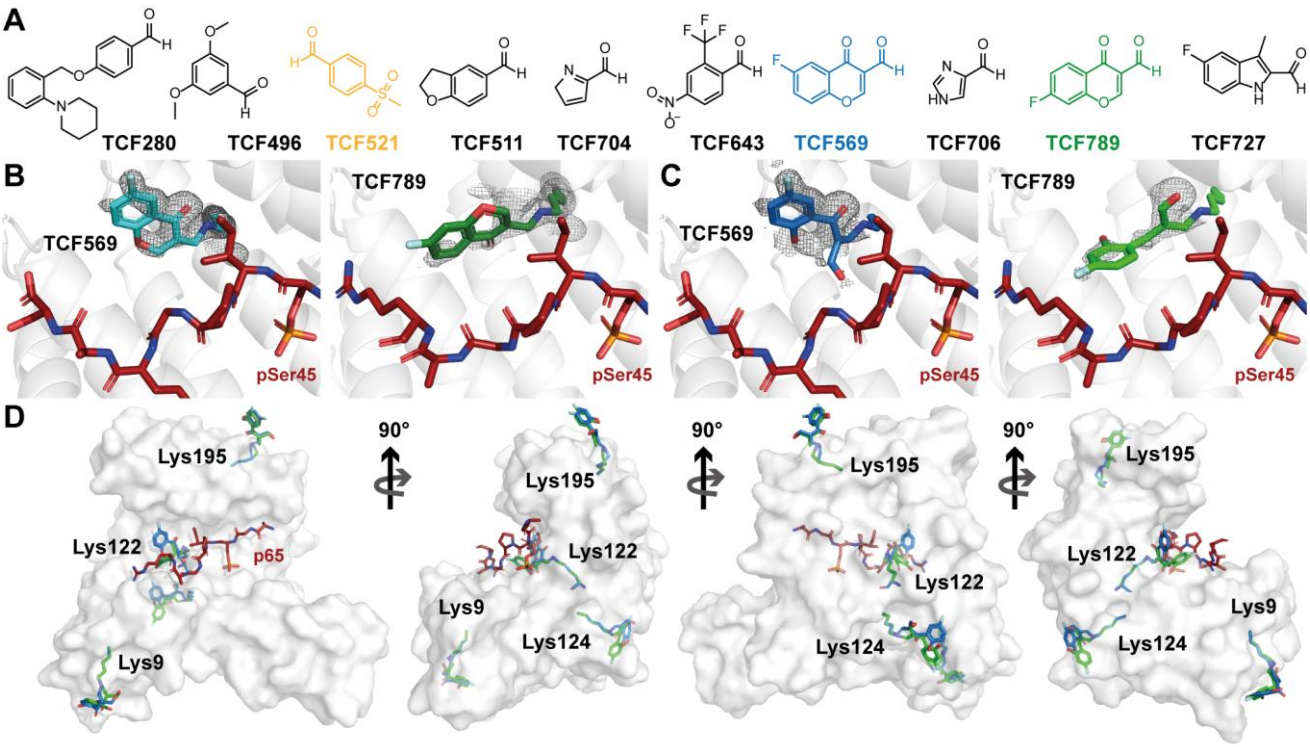

Figure S3: Screening of aldehydes for covalent targeting of Lys122. (A) Structures of the 10 initial fragments. The aldehydes were part of a fragment cocktail library assembled for the modulation of PPIs,[1] whereby hit identification was verified with singlet fragment soaks. TCF569 and TCF789 bind to Lys122 of 14-3-3 via Imine bond formation (B) or Michael addition (C). The 2Fo-Fc electron density (grey mesh) is contoured at 1σ. (D) TCF569 and TCF789 bind to at least four lysine residues of 14-3-3. 14-3-3 is shown as white cartoon or van-der Waals surface representation, p65 is shown as red sticks, TCF569 as green sticks and TCF789 as blue sticks.

Table S2. Data collection and refinement statistics for fragment/p65/14-3-3σΔC complexes. Collection statistics were calculated with aimless and refinement statistics were extracted using the "table 1" option of Phenix. TCF569 and TCF789 had a low coverage with electron density making an accurate interpretation of the binding pose and binding mode (imine formation or Michael addition) impossible. The crystal structures were therefore not uploaded to the PDB server. Statistics for the highest-resolution shell are shown in parenthesis.

	TCF521	**TCF569**	**TCF789**
PDB accession code	**6YOW**	**not submitted**	**not submitted**
X-ray source	P11, DESY	P11, DESY	P11, DESY
Data Collection			
Wavelength	1.033200	1.033200	1.033200
Resolution range	62.61 – 1.23 (1.26 – 1.23)	45.65 – 1.42 (1.46 – 1.42)	62.77 – 1.37 (1.41 – 1.37)
Space group	C2221	C2221	C2221
Unit cell			
a, *b*, *c* (Å)	82.5, 112.1, 62.6	82.337 112.408 62.834	82.210 112.116 62.771
α, β, γ (°)	90, 90, 90	90, 90, 90	90, 90, 90
Unique reflections	84336 (6167)	55271 (4037)	61169 (4467)
Multiplicity	8.6 (6.6)	8.9 (8.9)	8.9 (8.3)
Completeness (%)	100.0 (100.0)	100.0 (100.0)	100.0 (100.0)
Mean I/sigma(I)	14.3 (2.9)	17.0 (3.0)	13.6 (2.7)
R-merge	0.069 (0.513)	0.062 (0.593)	0.083 (0.638)
R-meas	0.073 (0.557)	0.065 (0.629)	0.088 (0.681)
R-pim	0.024 (0.214)	0.021 (0.210)	0.029 (0.235)
CC1/2	0.997 (0.855)	0.999 (0.862)	0.997 (0.810)
Refinement			
Reflections used in refinement	84307 (8343)	55241 (5404)	61135 (6063)
Reflections used for R-free	4352 (414)	2768 (274)	3069 (322)
R-work	0.1838 (0.2558)	0.1886 (0.2570)	0.1789 (0.2730)
R-free	0.2021 (0.2728)	0.2095 (0.2940)	0.2015 (0.2703)
Number of non-hydrogen atoms	2321	2167	2183
macromolecules	1951	1887	1891
ligands	11	62	57
solvent	359	218	235
RMS(bonds)	0.018	0.011	0.008
RMS(angles)	1.87	1.04	0.92
Ramachandran favored (%)	98.25	98.65	98.65
Ramachandran allowed (%)	1.75	1.35	1.35
Ramachandran outliers (%)	0	0.00	0
Rotamer outliers (%)	0.5	0.00	0
Clashscore	1.81	2.38	1.59
Average B-factor	17.64	24.06	24.4
macromolecules	15.41	22.35	21.94
ligands	23.13	45.62	60.31
solvent	29.59	32.74	35.42

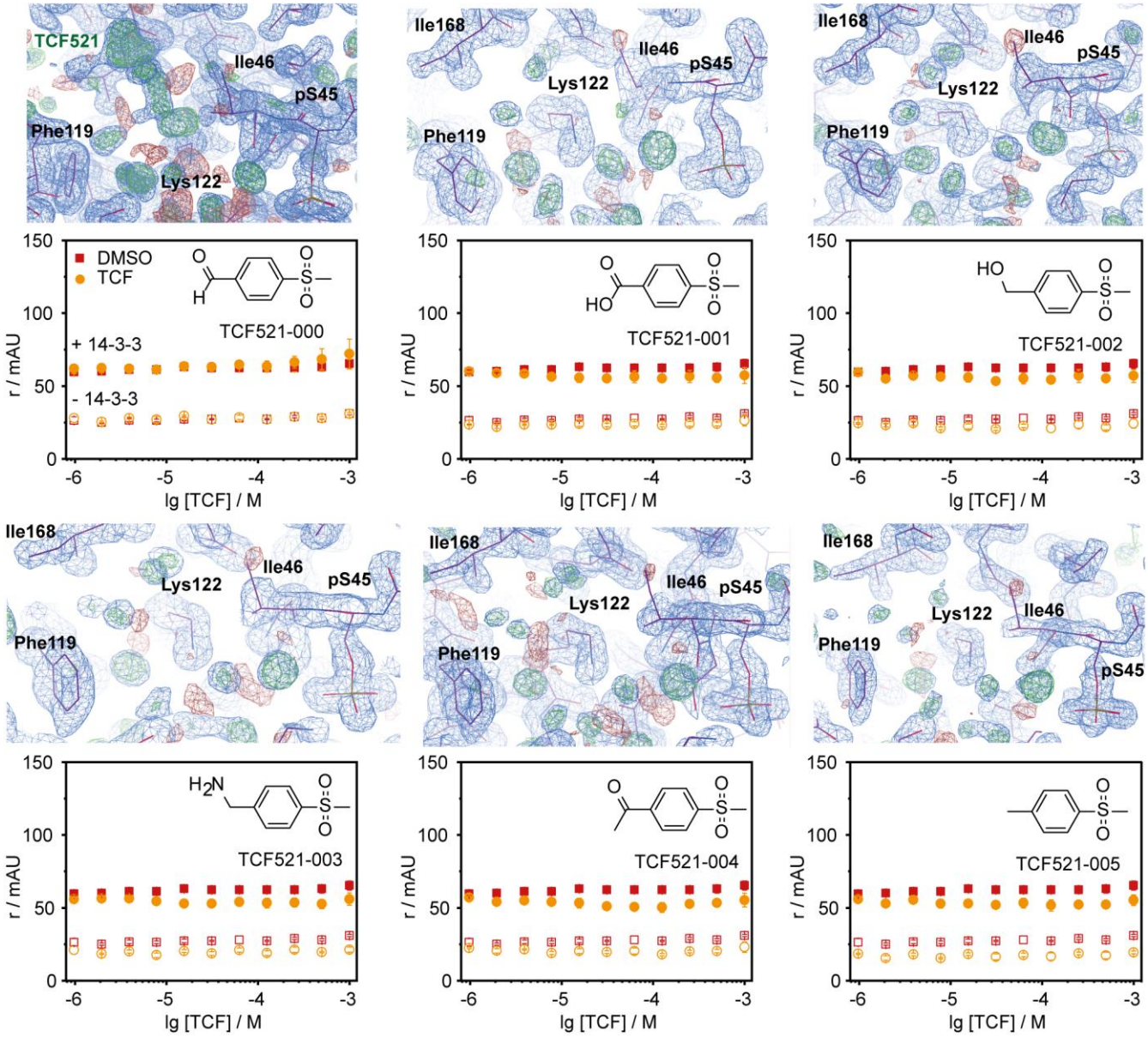

Figure S4: Replacement of aldehyde with diverse functional groups. The 2Fo-Fc electron density is contoured at 1σ. For FA assays, the compounds were titrated to 50 µM 14-3-3 and 100 nM of fluorescin-p65 (+14-3-3 protein) or to 100 nM fluorescin-p65 only (-14-3-3). Shown are mean +/- SD (n=3). Only TCF521 shows a minor increase in anisotropy at the highest concentration.

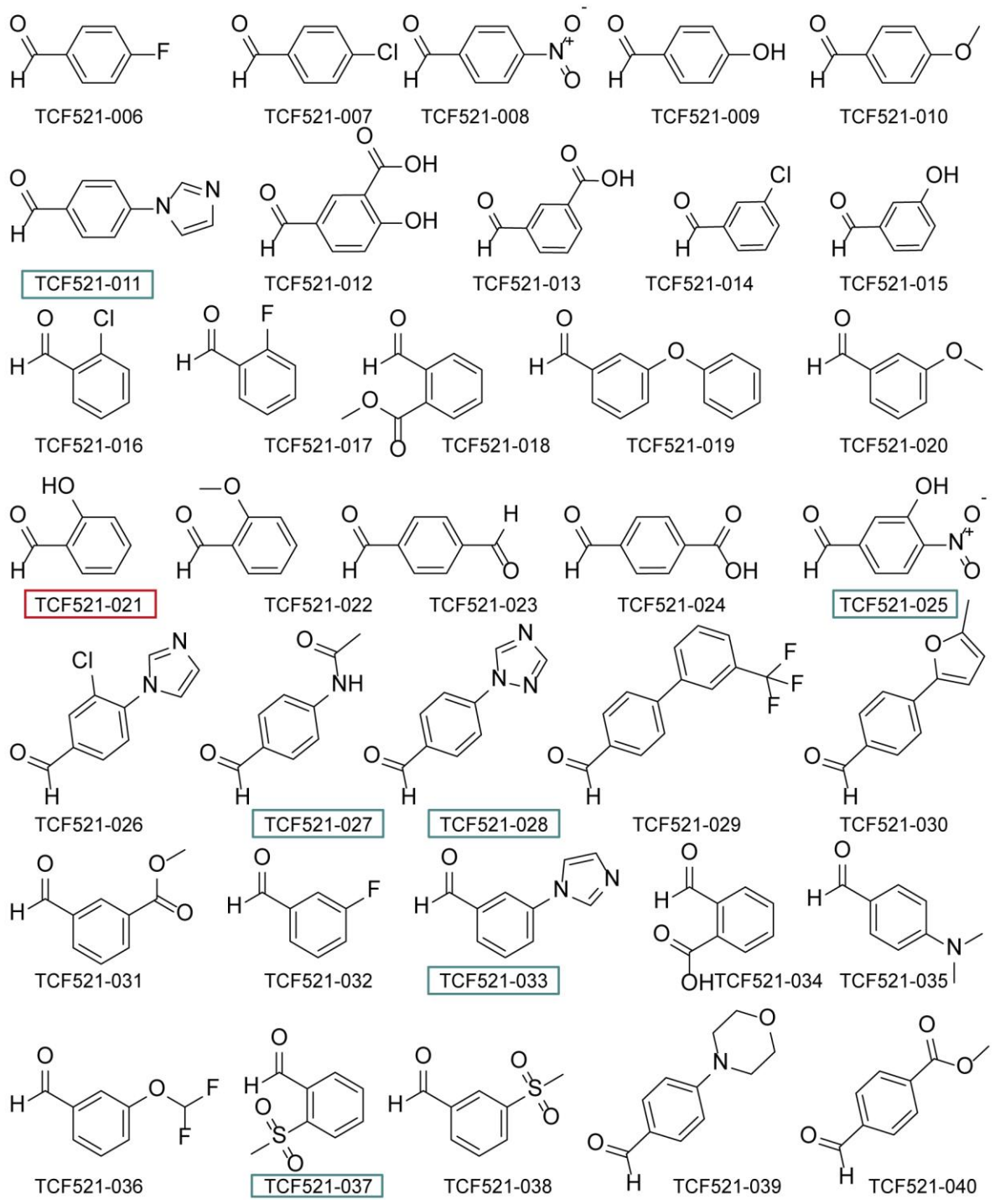

Figure S5: Extended aldehyde fragment library to investigate the contribution of an activation of the aldehyde. Fragments marked in cyan were detected in the electron denisty map of soaked p65/14-3-3 crystals (6/34 fragments, 18% hit rate), see Figure S5. The fragment marked in red induced crystal cracking, hence prevented data collection.

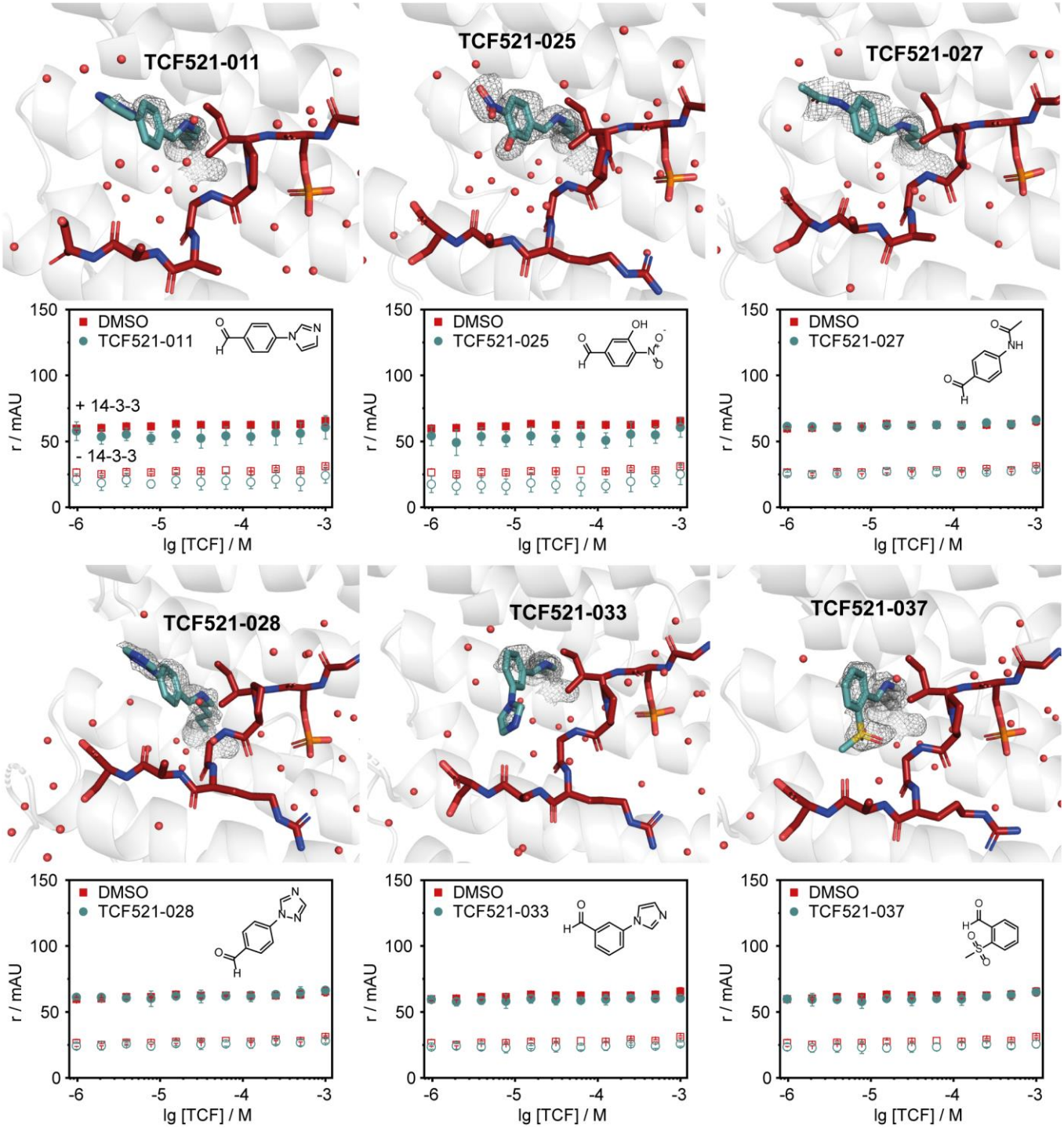

Figure S6: Crystal structure and FA assays for the indicated fragments. The fragments (cyan sticks) bind to the complex of 14-3-3 (white cartoon) and p65 (red sticks). The 2Fo-Fc electron density for the fragment is shown as grey mesh (contoured at 1σ). The compounds were titrated to 50 µM 14-3-3 and 100 nM of FITC-p65 (+14-3-3 protein) or to 100 nM fluorescin-p65 only (-14-3-3). Shown are mean +/- SD (n=3). None of the compounds were active in FA.

Table S3. Data collection and refinement statistics for fragment/p65/14-3-3σΔC complexes. Collection statistics were calculated with aimless and refinement statistics were extracted using the "table 1" option of Phenix. Statistics for the highest-resolution shell are shown in parenthesis.

	TCF521-011	TCF521-025	TCF521-027	TCF521-028	TCF521-033	TCF521-037
PDB ID	**6YP2**	**6YOY**	**6YOX**	**6YP3**	**6YP8**	**6YPL**

X-ray source	homesource	homesource	DLS* i03	homesource	homesource	homesource
Data Collection						
Wavelength	1.541870	1.541870	0.915870	1.541870	1.541870	1.541870
Resolution range	34.43 – 1.80 (1.83 – 1.80)	41.27 - 1.80 (1.85 - 1.80)	62.27 – 2.05 (2.08 – 2.05)	41.77 - 1.80 (1.84 - 1.80)	41.90 - 1.80 (1.84 - 1.80)	66.66 - 1.80 (1.84 - 1.80)
Space group	C2221	C2221	C2221	C2221	C2221	C2221
Unit cell						
a, *b*, *c* (Å)	82.5, 112.3, 62.6	82.5, 112.4, 62.6	82.2, 111.9, 62.3	82.5,112.2, 62.6	82.8, 112.8, 62.6	82.7, 112.7, 62.8
α, β, γ (°)	90, 90, 90	90, 90, 90	90, 90, 90	90, 90, 90	90, 90, 90	90, 90, 90
Unique reflections	26649 (1813)	26420 (1742)	18437 (1348)	27260 (1514)	27564 (1576)	27597 (1542)
Multiplicity	3.1 (2.5)	6.4 (5.5)	11.6 (8.3)	6.1 (4.1)	6.2 (4.7)	6.2 (4.7)
Completeness (%)	97.7 (88.3)	96.6 (87.5)	100.0 (100.0)	99.6 (93.8)	99.8 (97.6)	99.8 (95.9)
Mean I/sigma(I)	13.87 (2.50)	18.1 (4.0)	6.0 (1.8)	17.9 (2.8)	21.2 (3.5)	17.1 (3.2)
R-merge (all I+ & I-)	0.064 (0.248)	0.066 (0.238)	0.260 (0.950)	0.082 (0.350)	0.063 (0.286)	0.071 (0.289)
R-meas (all I+ & I-)	0.077 (0.306)	0.072 (0.262)	0.272 (1.014)	0.090 (0.399)	0.069 (0.321)	0.077 (0.325)
R-pim (all I+ & I-)	0.040 (0.177)	0.028 (0.108)	0.078 (0.348)	0.036 (0.187)	0.027 (0.143)	0.031 (0.146)
CC1/2	0.997 (0.918)	0.999 (0.972)	0.994 (0.887)	0.998 (0.886)	0.999 (0.943)	0.999 (0.947)
Refinement						
Reflections used in refinement	26631 (2492)	26405 (2323)	18367 (1799)	27240 (2579)	27543 (2665)	27572 (2637)
Reflections used for R-free	1337 (120)	1336 (109)	894 (86)	1382 (119)	1397 (120)	1403 (125)
R-work	0.1757 (0.2332)	0.1862 (0.2085)	0.1971 (0.3041)	0.1808 (0.2417)	0.1910 (0.2598)	0.1959 (0.2688)
R-free	0.2196 (0.3004)	0.2338 (0.2681)	0.2348 (0.2752)	0.2152 (0.2766)	0.2278 (0.3011)	0.2293 (0.3180)
Number of non-hydrogen atoms	2280	2183	2152	2287	2245	2230
macromolecules	1927	1877	1908	1950	1945	1937
ligands	13	12	14	13	13	12
solvent	340	294	230	324	287	281
RMS(bonds)	0.009	0.005	0.012	0.004	0.004	0.003
RMS(angles)	0.88	0.7	1.34	0.62	0.62	0.62
Ramachandran favored (%)	98.3	98.24	97.45	98.3	97.87	97.44
Ramachandran allowed (%)	1.7	1.76	2.55	1.7	2.13	2.56
Ramachandran outliers (%)	0	0	0	0	0	0
Rotamer outliers (%)	0	1.55	0	0	0	0
Clashscore	1.84	0.81	1.06	1.82	2.34	3.65
Average B-factor	15.86	15.35	33.86	15.87	17.47	16.85
macromolecules	13.96	13.94	32.91	14.28	16.07	15.58
ligands	43.04	23.06	58.48	39.03	50.18	33.56
solvent	25.62	23.98	40.24	24.51	25.43	24.9

*DLS: diamond light source

Table S4. Data collection and refinement statistics for fragment/p65/14-3-3σΔC complexes. Collection statistics were calculated with aimless and refinement statistics were extracted using the "table 1" option of Phenix. Statistics for the highest-resolution shell are shown in parenthesis.

	TCF521-123	TCF521-129
PDB accession code	**6YPY**	**6YQ2**
X-ray source	Diamond Light Source i24	Diamond Light Source i24
Data Collection		
Wavelength (Å)	0.968620	0.968620
Resolution range	56.22 – 1.40 (1.42 – 1.40)	66.59 – 1.40 (1.42 – 1.40)
Space group	C2221	C2221
Unit cell		
a, *b*, *c* (Å)	82.598 112.444 62.555	82.781 112.095 62.619
α, β, γ (°)	90.000 90.000 90.000	90.000 90.000 90.000
Unique reflections	57549 (2797)	57580 (2914)
Multiplicity	1.9 (1.9)	1.9 (1.9)
Completeness (%)	100.0 (100.0)	100.0 (100.0)
Mean I/sigma(I)	11.1 (4.3)	12.2 (2.1)
R-merge	0.046 (0.157)	0.024 (0.283)
R-meas	0.065 (0.223)	0.034 (0.400)
R-pim	0.046 (0.157)	0.024 (0.283)
CC1/2	0.993 (0.922)	0.999 (0.780)
Refinement		
Reflections used in refinement	57539 (5657)	57541 (5657)
Reflections used for R-free	2913 (262)	2913 (262)
R-work	0.1712 (0.2162)	0.2717 (0.3455)
R-free	0.1925 (0.2333)	0.2793 (0.3417)
Number of non-hydrogen atoms	2319	2222
macromolecules	1967	1919
ligands	19	18
solvent	333	285
RMS(bonds)	0.009	0.01
RMS(angles)	1.01	1.04
Ramachandran favored (%)	98.28	97.79
Ramachandran allowed (%)	1.72	1.77
Ramachandran outliers (%)	0	0.44
Rotamer outliers (%)	0	0
Clashscore	2.05	2.88
Average B-factor	15.31	20.96
macromolecules	13.55	19.35
ligands	11.56	27.41
solvent	25.89	31.39

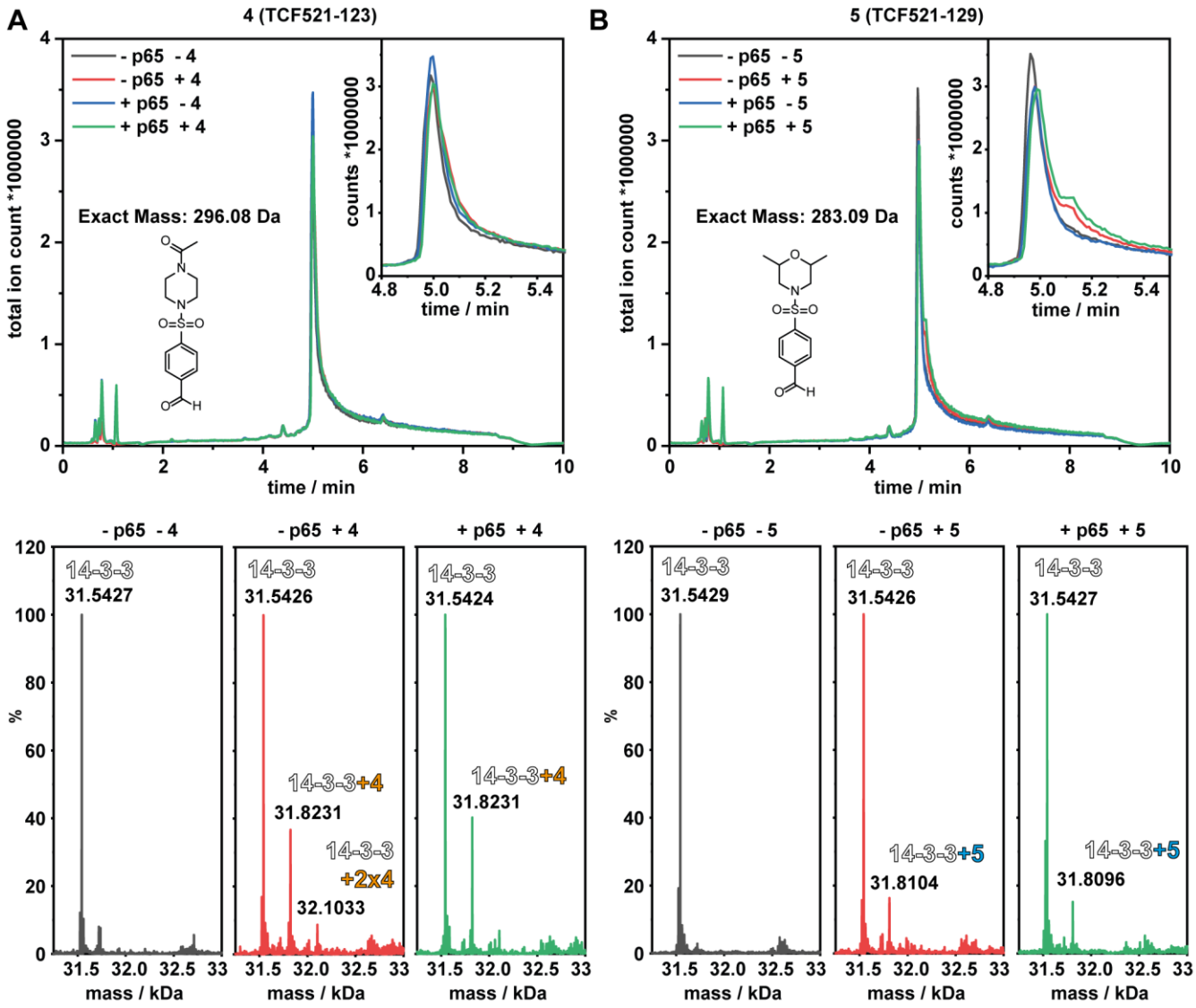

Figure S7: Mass spectroscopic analysis of 4 and 5 binding to 14-3-3. (A) Chromatogram (upper panel) of 14-3-3γ (5 µM) with/without the p65 peptide (1 mM) and/or 4 (500 µM). The exact mass and chemical structure of the uncoupled compound is indicated. The corresponding deconvoluted mass/z spectra (lower panel, normalized to the highest peak) show mainly one reacted compound per protein with a minor peak with two compounds per 14-3-3. Following imine formation and reductive amination an additional mass of 280 Da per compound is expected resulting in theoretical mass of 31˙542.5 Da (14-3-3γ), 31˙822.9 Da (14-3-3γ+4) and 32˙102.6 Da (14-3-3γ+2x4). (B) Chromatogram (upper panel) and deconvoluted mass/z spectra (lower panel, normalized to the highest peak) for 14-3-3γ (5 µM) with/without the p65 peptide (1 mM) and/or 4 (500 µM). Details as described in A. After imine formation and reductive amination an additional mass of 267 Da per coupled 5 is expected resulting in theoretical mass of 31˙542.5 Da (14-3-3γ), 31˙809.5 Da (14-3-3γ+5) and 32˙076.5 Da (14-3-3γ+2x5).

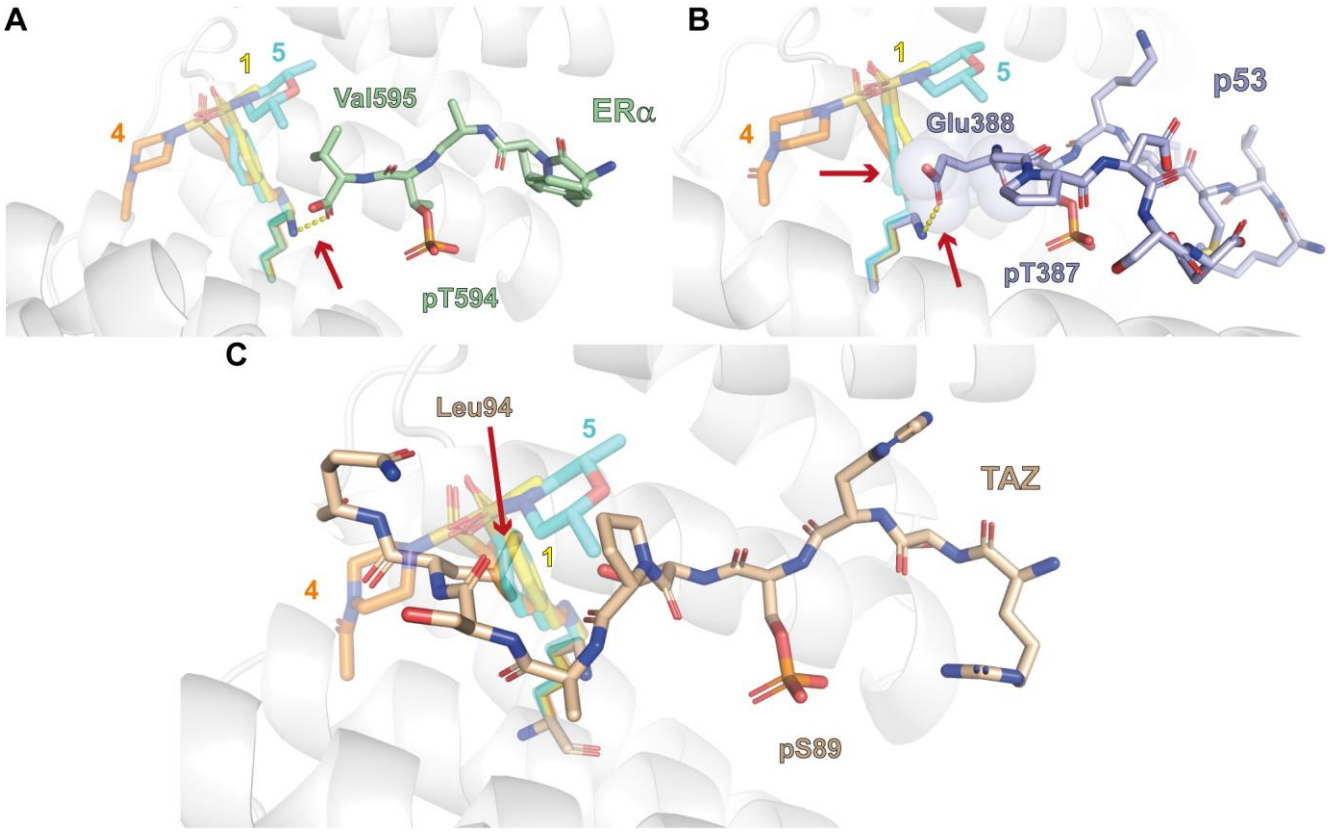

Figure S8: Overlay of the crystal structures of 1,4 and 5 with ERα-, p53- and TAZ-peptide in complex with 14-3-3. (A) Val595 of the ERα-peptide (green sticks) is hydrogen bonding with Lys122, thereby preventing imine formation of the benzaldehydes (transparent sticks) (ERα/14-3-3 complex PDB: 4JC3). **(B)** Glu388 of the p53 peptide (violet sticks) is causing a steric clash with the benzaldehyde core of 1,4 and 5 (transparent sticks) in addition to its hydrogen bonding to Lys122 (p53/14-3-3 complex PDB: 5MOC). **(C)** Leu94 of the TAZ-peptide (beige sticks) would cause a steric clash with all three compounds (transparent sticks)(TAZ/14-3-3 complex PDB: 5N75). 14-3-3 is shown as white cartoon for all.

Material and Methods

Protein Expression and Purification

14-3-3 proteins were expressed in BL21(DE3) cells with pPROEX HTb vectors encoding for the indicated isoforms. Cells were grown to an OD_{600}=0.8-1 in TB media and expression was induced with 0.4mM IPTG overnight at 18°C. After harvesting the cells by centrifugation (10.000 xg, 15 min), they were resuspended in lysis buffer (50 mM Tris/HCl pH8, 300 mM NaCl, 12.5 mM imidazole, 2 mM β-mercaptoethanol). A homogenizer was used for cell lysis, the lysate was cleared via centrifugation (40.000 xg, 30min). The cleared lysate was applied to Ni-NTA-columns and eluted with 250 mM imidazole (50 mM Tris/HCl pH8, 300 mM NaCl, 250 mM imidazole, 2 mM β-mercaptoethanol). For the full length 14-3-3γ, the imidazole was removed via dialysis, the protein rebuffered (25mM HEPES pH7.5, 100mM NaCl, 10mM $MgCl_2$, 0.5mM Tris(2-carboxyethyl)phosphine) and stored at -80°C. For the 14-3-3σΔC (last 17 amino acids of flexible C-terminus were removed) for crystallography, the His6-tag was removed following standard procedures of TEV cleavage; the TEV was removed with Ni-NTA-columns. For highest purity necessary for crystallography, the protein was additionally applied to size exclusion chromatography (20 mM HEPES pH7.5, 150 mM NaCl, 2 mM β-mercaptoethanol) and stored at -80°C.

Note to the use of 14-3-3 isoforms: 14-3-3σΔC was only used for crystallography because of its enhanced potential to grow high resolution crystals. For all other techniques the 14-3-3γ isoform was used due to its beneficial binding to the p65 epitope.[2] All residues of the p65/14-3-3 interface are conserved throughout all human 14-3-3 isoforms, so that the observed contacts in the crystal structures are translatable to all isoforms.

X-Ray Crystallography

Binary crystals with NF-κBp65 peptide (Sequence: EGRSAG pS_{45} IPGRRS, C-terminus: amidation; N-terminus: acetylation)[2] and 14-3-3σΔC were grown as follows: 14-3-3σΔC at a concentration of 12 mg/ml was mixed in a 1:2 ratio with the acetylated NF-κBp65 peptide in 20 mM HEPES pH7.5, 2 mM $MgCl_2$, 2 mM β-mercaptoethanol and incubated at 4°C overnight. Then it was mixed in 1:2 ratio with precipitation buffer (95 mM HEPES pH7.5, 27-28% PEG400, 190 mM $CaCl_2$, 5% glycerol) in the wells of a hanging drop crystallography plate. The reservoir was filled with 500 µL precipitation buffer. Crystals grew within two weeks and were directly flash frozen in liquid nitrogen for data acquisition.

For soaking experiments compounds in DMSO stock solutions were directly added to fully grown crystals to a final compound concentration of 10 mM (≤1% DMSO) in the crystal solution. After seven days the crystals were harvested and measured as indicated in Table S2, S3 and S4 either on a home source, P11 beamline of PetraIII (DESY campus, Hamburg, Germany) or i-03/i-24 beamline of the diamond light source (Oxford, UK). For data integration the xia2/DIALS pipeline[3] was utilized followed by molecular replacement with MolRep[4,5] using the NF-κBp65/14-3-3 binary structure as search model (PDB ID: 6QHL). Model building was done in iterative cycles with Coot[6], Refmac5[7] and phenix.refine[8]. For ligand preparation, the fragment SMILES were transformed to 3D models using elbow of the phenix suite[8]. Figures were generated with PyMOL© (V2.0.6, Schrodinger LLC). The crystal structures were uploaded to the PDB server with the following PDB IDs: 6YOW, 6YP2, 6YOY, 6YOX, 6YP3, 6YP8, 6YPL, 6YPY, 6YQ2.

Mass Spectrometry

Reductive amination of **4** (TCF521-123) and **5** (TCF521-129) and following LC/MS analysis of the complex was performed as follows: 50 µM of 14-3-3γ and/or 1 mM of monovalent p65 peptide and 500 µM of compound were incubated in 10 mM HEPES pH 7.4, 150 mM NaCl for 1h at RT, then an 1000x excess of $NaBH_3CN$ was added (fresh stock solution with 6 mg/ml). The mixture was incubated for 1h at RT before the reaction was stopped with 0.1% formic acid, diluting the mixture by 1:100.

For all the samples were applied to a hybrid quadrupole time-of-flight (QTOF) LC/MS system, with 1 µL injection volume. The chromatogram was measured on an Agilent Polaris C18-A 100x2.00mm column over 8 min with a water/acetonitrile (+0.1% formic acid) gradient of 15-60% acetonitrile/0.1% formic acid followed by 2 min washing with 15% acetonitrile acetonitrile/0.1% formic acid (flowrate 0.3ml/min, column temperature 60ºC). For MS data acquisition a full scan with 150-2000 m/z was performed and data analysis was performed with the MassLynx software. For deconvolution of the mass/z spectra the MaxEnt1 function of the MassLynx software was applied to the 4 most abundant peaks of the mass distributions. The output mass range was set to 30-40kDa with a resolution of 0.1 Da/channel. As damage model the “simulated isotope pattern” was applied, whereby the blur width was determined by measuring the peak width of the most abundant peak at half of its height (typically 0.3 Da). All graphs were prepared with OriginLab 2019.

Fluorescence Anisotropy Assays

Fluorescence Anisotropy was measured in Corning 384 well plates (black, round bottom, low binding) with the Tecan Infinite 500 plate reader (FITC dye: excitation 485 nm, emission 535 nm; TAMRA dye: excitation 535 nm, emission 590 nm) in FA buffer (10 mM HEPES pH 7.4, 150 mM NaCl, 0.1% Tween20). The plates were measured after 3h incubation at RT. The concentration of the peptide coupled to the fluorescent tracer was kept constant as follows: FITC-βAla-p65 c = 100 nM, TAMRA-Ahx-p53 peptide c = 10 nM, FITC-βAla-TAZ c = 10 nM, FITC- O1Pen -ERα c= 10 nM. Peptide sequences are listed in Table S5.

For compound titrations, the 14-3-3γ concentrations was constant at concentration of 1/3 of the K_D of the binary complex (assay concentration for p65: 50 µM, TAZ: 0.1 µM, Era: 0.1 µM, p53: 0.3 µM) and the compound was titrated in a 1:1 dilution series with a highest concentration of 2 mM.

For protein titrations, the compound and peptide concentration were constant as indicated; the protein was titrated in a 1:1 dilution series starting from 400 µM. For 2D titrations the compound was diluted in a 1:1 dilution series in DMSO prior to the protein titrations to keep the DMSO concentration constant throughout the assay. The K_D of the DMSO control was calculated using the average and standard deviation of fitted EC_{50} values over two independent measurements each with three technical replicates.

Table S5: Overview of peptide sequences. Shown are the names of the peptides as used in this manuscript, the N-terminal fluorescent dyes and the corresponding linker, the sequence and the references.

Peptide name	N-terminal modification	Sequence	reference
p65 monovalent	FITC-βAla	EGRSAG pS45 IPGRRS	[2]
p65 bivalent	FITC-βAla	EGRSAG pS45 IPGRRSGSGGGSGPSDREL pS EPMEFQ	[2]
TAZ	FITC-βAla	RSH pS89 SPASLQ	[9]
p53	TAMRA-Ahx	SRAHSSHLKSKKGQSTSRHKKLMFK pT387 EGPDSD - COOH	[10]
ERα	FITC-O1Pen	AEGFPA pT594 V-COOH	[11]

General information

Except for TCF280 (Figure S2), TCF521-123 and TCF521-129 all aldehydes shown are commercially available. All commercial chemicals were used as received, considering the purity reported from the supplier. The dry powder was stored in a fridge at +4 °C and DMSO stock solutions were stored at -30 °C.
Reagents were used without further purification unless otherwise noted.

TLC analysis was performed on TLC aluminum sheets, silica gel layer, ALUGRAM SIL G UV254, 20x20 cm by MACHEREY-NAGEL. TLC plates were analysed by UV fluorescence (254 nm).

UHPLC-MS analysis was performed using UPLC Agilent Technologies 1290 Infinity coupled with Agilent Technologies 6120 Quadrupole LC/MS DAD detector.
Column: ACQUITY UHPLC BEH C18 (1.7 µm) 2.1 mm x 50 mm
Temperature: 40 °C.
Detection: DAD + MS/6120 Quadrupole.
Injected volume: 1µL
Flow: 1.2 mL/min.
Solvent A: Water + 0.1% Formic Acid.
Solvent B: Acetonitrile + 0.1% Formic Acid.
Gradient: 0 min 2% B; 0.2 min 2% B; 2.0 min 98% B; 2.2 min 98% B; 2.21 min 2% B; 2.5 min 2% B.

Preparative HPLC was performed using UPLC Agilent Technologies 1260 Infinity coupled with Agilent Technologies 6120 Quadrupole LC/MS.
Column: Waters XBridge Prep C18 5 µm OBD 19 x 150 mm.
Detection: DAD + MS/6120 Quadrupole.
Flow: 32 mL/min.
Solvent A: Water + 0.1% Formic Acid.
Solvent B: Acetonitrile + 0.1% Formic Acid.
Gradient: 0 min 77% A / 23% B; 1 min 77% A / 23% B; 9 min 16% A / 84% B; 9.01 min 2% A / 98% B; 11 min 2% A / 98% B.

^{1}H NMR and ^{13}C NMR spectra were recorded on a Bruker 300 MHz spectrometer at ambient temperature.
The chemical shifts are listed in ppm on the δ = scale and coupling constants were recorded in Hertz (Hz). Chemical shifts are calibrated relative to the signals corresponding of the non-deuterated solvent ($CHCl_3$: δ = 7.26 ppm for 1H and 77.16 for 13C).
Abbreviations are used in the description of NMR data as follows; chemical shift (δ = ppm), multiplicity (s = singlet, d = doublet, t = triplet, m = multiplet, bs = broad singlet), coupling constant (J = Hz).

Synthesis of undescribed products

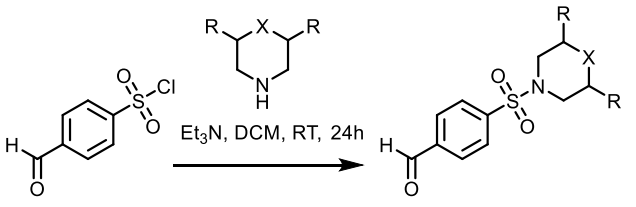

4 (34 %); X = NAc, R=H
5 (32 %); X = O, R=CH_3

Scheme 1. The synthesis of 4-formylbenzenesufonamides (Scheme as shown in main text, here for clarity).

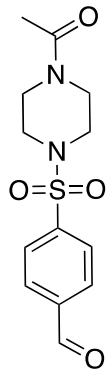

4-[(4-acetylpiperazin-1-yl)sulfonyl]benzaldehyde (**4**, TCF521-123)

To a solution of 0.29 mmol (1 Eq.) 1-Acetylpiperazine in 1 ml of DCM were added 0.88 mmol (3 Eq.) of Triethylamine. After stirring at room temperature for 10 min., a solution of 0.29 mmol (1 Eq.) 4-formylbenzene-1-sulfonyl-chloride in 1 ml of DCM was added. The reaction was stirred at room temperature for 24 hours. After complete consumption of the starting materials - monitored by TLC (DCM/MeOH 9:1) and UHPLC-MS, 1ml of saturated $NaHCO_3$ solution was added to the reaction mixture. After separation, the organic layer was dried and concentrated under pressure. The compound was purified by preparative HPLC. Obtained 30 mg (34% yield) of **4 (TCF521-123)** with purity 99% by UHPLC-MS as a white solid. UHPLC-MS (ESI + APCI) m/z calcd. for $C_{13}H_{16}N_2O_4S$ $[M+H]^+$ = 297. Found: 297. Retention time: 1.01 min. ^{1}H NMR (300 MHz, $CDCl_3$) δ = 10.11 (s, 1H), 8.05 (d, *J* = 8.44 Hz, 2H), 7.90 (d, *J* = 8.30 Hz, 2H), 3.70 (t, 2H), 3.55 (t, 2H), 3.04 (m, 4H), 2.02 (s, 3H) ppm. ^{13}C NMR (75 MHz, $CDCl_3$) δ = 190.4, 166.6, 140.5, 139.0, 130.1, 128.1, 45.9, 45.6, 45.5, 40.5, 21.0ppm.

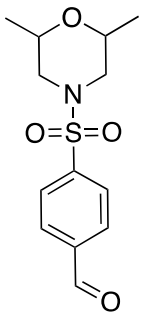

4-[(2,6-dimethylmorpholin-4-yl)sulfonyl]benzaldehyde (**5**, TCF521-129)

To a solution of 0.29 mmol (1 Eq.) 2.6-Dimethylmorpholine in 1 ml of DCM were added 0.88 mmol (3 Eq.) of Triethylamine. After stirring at room temperature for 10 min., a solution of 0.29 mmol (1 Eq.) 4-formylbenzene-1-sulfonyl-chloride in 1 ml of DCM was added. The reaction was stirred at room temperature for 24 hours. After complete consumption of the starting materials - monitored by TLC (DCM/MeOH 9:1) and UHPLC-MS, 1ml of saturated $NaHCO_3$ solution was added to the reaction mixture. After separation, the organic layer was dried and concentrated under pressure. The compound was purified by preparative HPLC. Obtained 26.6 mg (32% yield) of **5 (TCF521-129)** with purity 99% by UHPLC-MS as a white solid. UHPLC-MS (ESI + APCI) m/z calcd. for $C_{13}H_{17}NO_4S$ $[M+H]^+$ = 284. Found: 284. Retention time: 1.29 min. ^{1}H NMR (300 MHz, $CDCl_3$) δ = 10.12 (s, 1H), 8.06 (d, *J* = 8.47 Hz, 2H), 7.91 (d, *J* = 8.26 Hz, 2H), 3.70 (m, 2H), 3.60 (d, *J* = 10.14 Hz, 2H), 1.97 (m, 2H), 1.13 (d, *J* = 6.27 Hz, 6H) ppm. ^{13}C NMR (75 MHz, $CDCl_3$) δ = 190.5, 140.6, 138.8, 130.0, 128.1, 71.1, 50.5, 18.4 ppm.

^{1}H NMR (300 MHz, $CDCl_3$) 4-[(4-acetylpiperazin-1-yl)sulfonyl]benzaldehyde (4, TCF521-123):

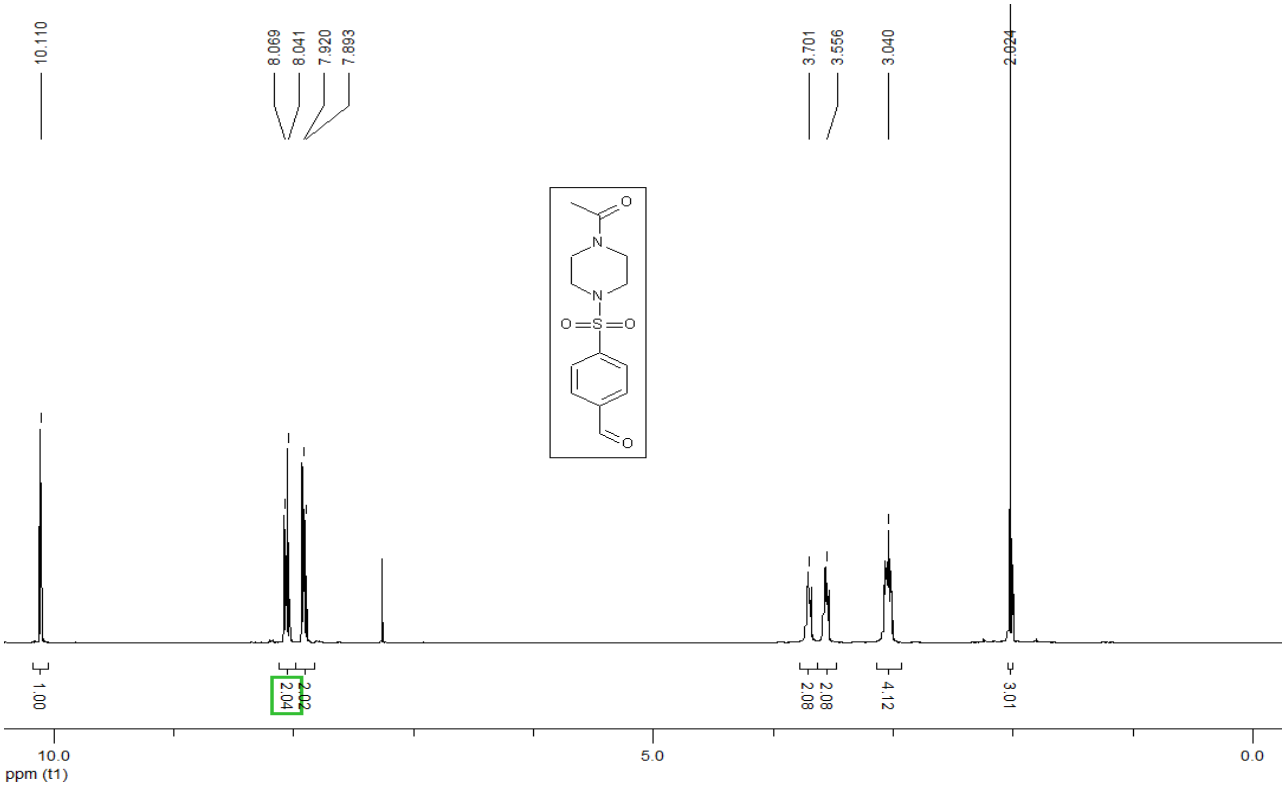

^{13}C NMR (75 MHz, $CDCl_3$) 4-[(4-acetylpiperazin-1-yl)sulfonyl]benzaldehyde (4, TCF521-123):

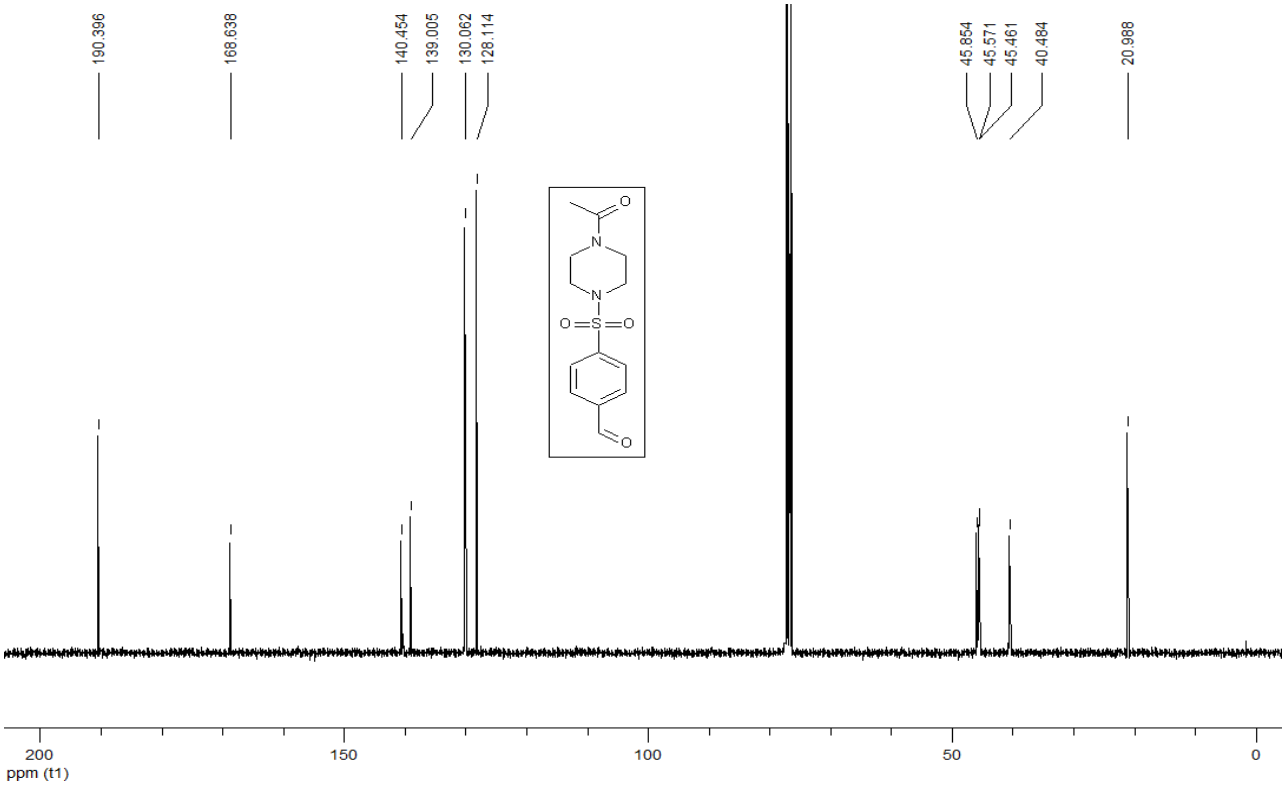

^{1}H NMR (300 MHz, $CDCl_3$) 4-[(2,6-dimethylmorpholin-4-yl)sulfonyl]benzaldehyde (5, TCF521-129):

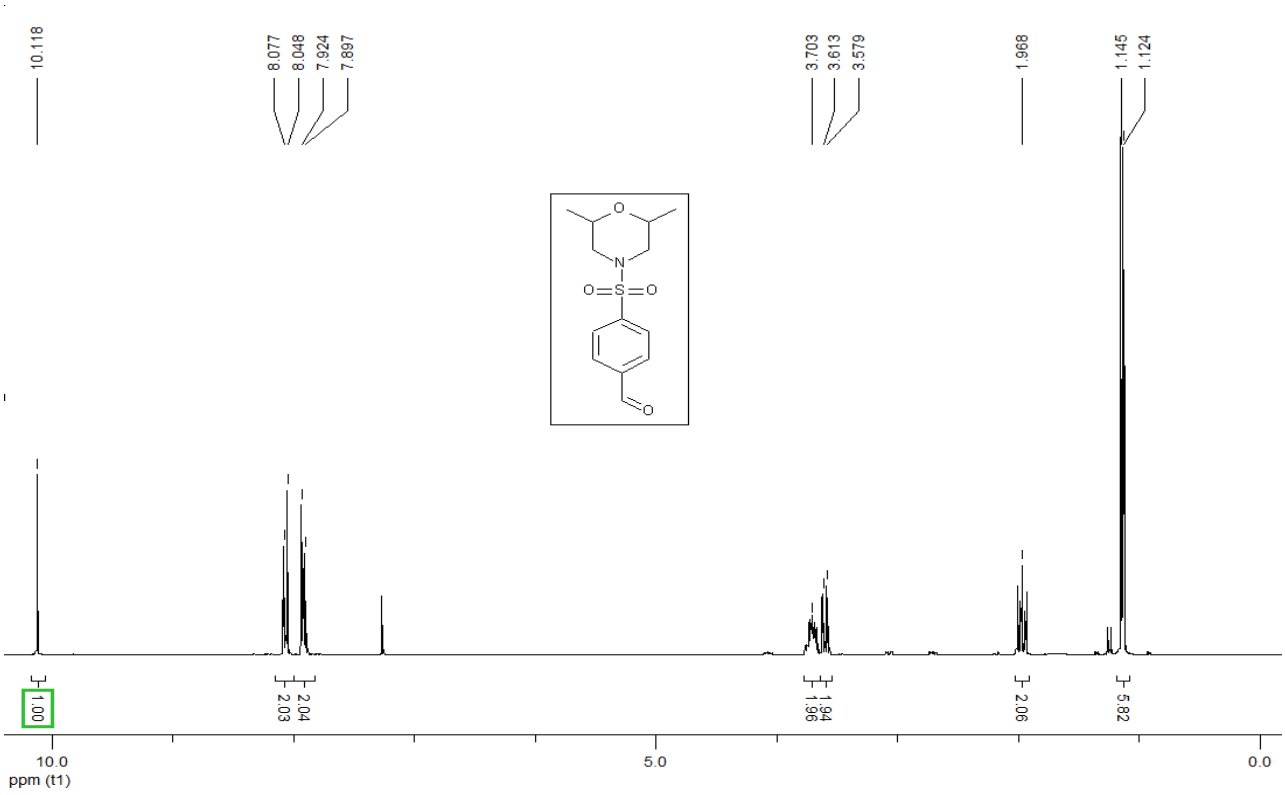

^{13}C NMR (75 MHz, $CDCl_3$) 4-[(2,6-dimethylmorpholin-4-yl)sulfonyl]benzaldehyde (5, TCF521-129):

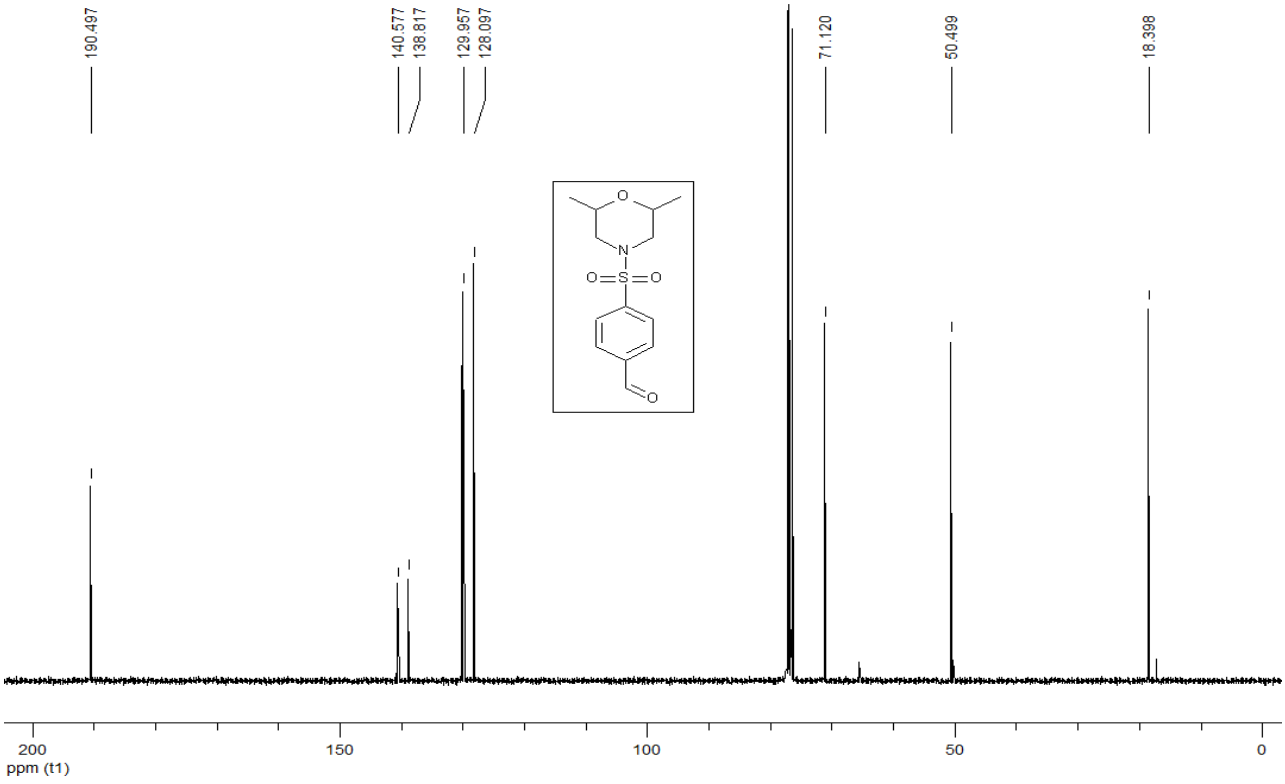

References

[1] Valenti D, Neves JF, Cantrelle F-X, Hristeva S, Lentini Santo D, Obšil T, Hanoulle X, Levy LM, Tzalis D, Landrieu I, Ottmann C, *Medchemcomm* **2019**, *10*, 1796–1802, DOI:10.1039/c9md00215d.
[2] Wolter M, de Vink P, Neves JF, Srdanovic S, Higuchi Y, Kato N, Wilson AJ, Landrieu I, Brunsveld L, Ottmann C, *J. Am. Chem. Soc.* **2020**, DOI:10.1021/jacs.0c02151.
[3] Clabbers MTB, Gruene T, Parkhurst JM, Abrahams JP, Waterman DG, *Acta Cryst. D.* **2018**, *74*, 506–518, DOI:10.1107/S2059798318007726.
[4] Lebedev AA, Vagin AA, Murshudov GN, *Acta Cryst. D.* **2008**, *64*, 33–39, DOI:10.1107/S0907444907049839.
[5] Vagin A, Teplyakov A, *Acta Cryst. D.* **2010**, *66*, 22–25, DOI:10.1107/S0907444909042589.
[6] Emsley P, Cowtan K, *Acta Cryst D* **2004**, *60*, 2126–2132, DOI:10.1107/S0907444904019158.
[7] Murshudov GN, Skubák P, Lebedev AA, Pannu NS, Steiner RA, Nicholls RA, Winn MD, Long F, Vagin AA, *Acta Cryst. D.* **2011**, *67*, 355–367, DOI:10.1107/S0907444911001314.
[8] Adams PD, Afonine PV, Bunkóczi G, Chen VB, Davis IW, Echols N, Headd JJ, Hung L-W, Kapral GJ, Grosse-Kunstleve RW, McCoy AJ, Moriarty NW, Oeffner R, Read RJ, Richardson DC, Richardson JS, Terwilliger TC, Zwart PH, *Acta Cryst. D.* **2010**, *66*, 213–221, DOI:10.1107/S0907444909052925.
[9] Sijbesma E, Hallenbeck KK, Leysen S, de Vink PJ, Skóra L, Jahnke W, Brunsveld L, Arkin MR, Ottmann C, *J. Am. Chem. Soc.* **2019**, *141*, 3524–3531, DOI:10.1021/jacs.8b11658.
[10] Doveston RG, Kuusk A, Andrei S, Leysen S, Cao Q, Castaldi P, Hendricks A, Chen H, Boyd H, Ottmann C, *FEBS Lett* **2017**, *591*, 2449–2457, DOI:10.1002/1873-3468.12723.
[11] Vink PJ de, Andrei SA, Higuchi Y, Ottmann C, Milroy L-G, Brunsveld L, *Chem. Sci.* **2019**, *10*, 2869–2874, DOI:10.1039/C8SC05242E.